Measurement and Modeling of Ground-Level Ozone Concentration in Catania, Italy using Biophysical Remote Sensing and GIS

[1]Fabio Famoso, [2]Jeffrey Wilson, [3]Pietro Monteforte,
[4]Rosario Lanzafame, [5]Sebastian Brusca and [6]Vijay Lulla

[1]PhD, University of Catania, Catania, Italy.
[2]PhD, Department of Geography, Indiana University-Purdue University Indianapolis, Indiana.
[3]University of Catania, Catania, Italy.
[4]PhD, University of Catania, Catania, Italy.
[5]PhD, Department of Engineering, University of Messina, Messina, Italy.
[6]PhD, Department of Geography, Indiana University-Purdue University Indianapolis, Indiana.

[1]Orcid: 0000-0003-3880-0292 & Scopus ID: 56029382400

Abstract

This experimental study examined spatial variation of ground level ozone (O_3) in the city of Catania, Italy using thirty passive samplers deployed in a 500-m grid pattern. Significant spatial variation in ground level O_3 concentrations (ranging from 12.8 to 41.7 $\mu g/m^3$) was detected across Catania's urban core and periphery. Biophysical measures derived from satellite imagery and built environment characteristics from GIS were evaluated as correlates of O_3 concentrations. A land use regression model based on four variables (land surface temperature, building area, residential street length, and distance to the coast) explained 74% of the variance (adjusted R^2) in measured O_3. The results of the study suggest that biophysical remote sensing variables are worth further investigation as predictors of ground level O_3 (and potentially other air pollutants) because they provide objective measurements that can be tested across multiple locations and over time.

Nomenclature

Variable	Unit of Measure	Description
LST_{200sc}	°K	Land surface temperature mean in 200m semicircular buffer
LST_{150sc}	°K	Land surface temperature mean in 150m semicircular buffer
ALB_{200c}	Unitless Index	Albedo mean in 200m circular buffer
LST_{100sc}	Unitless Index	Land surface temperature mean in 100m semicircular buffer
ALB_{150c}	Unitless Index	Albedo mean in 150m circular buffer
ALB_{100c}	Unitless Index	Albedo mean in 100m circular buffer
ALB_{200sc}	Unitless Index	Albedo mean in 200m semicircular buffer
LST_{200c}	°K	Land surface temperature mean in 200m circular buffer
LST_{150c}	°K	Land surface temperature mean in 150m circular buffer
LST_{100c}	°K	Land surface temperature mean in 100m circular buffer
LST_{50sc}	°K	Land surface temperature mean in 50m semicircular buffer
ALB_{150sc}	Unitless Index	Albedo mean in 150m semicircular buffer
LST_{50c}	°K	Land surface temperature mean in 50m circular buffer
Coast	[m]	Distance to coast
$Rlength_{50c}$	[m]	Residential road length in 50m circular buffer
$Buildings_{50c}$	[m^2]	Buildings area in 50m circular buffer

INTRODUCTION

Urban air pollution negatively affects human health, quality of life, and ecosystem functions. Ground-level ozone (O_3) is among the pollutants of concern because of its toxicity to lung tissue, exacerbation of bronchial inflammation and asthmatic symptoms, in addition to other health impacts (D'Amato et al., 2010; Al-Heglan et al., 2011; Jerrett et al., 2017). Ground-level O_3 can also decrease photosynthetic activity, thereby reducing ecosystem services of vegetation (Calfapietra et al., 2016).

The current experimental study was conducted in the Italian city of Catania where changes in national and EU policies have led to a reduction in the number of continuous air quality monitoring stations. Seventeen continuous monitoring sites

This is the author's manuscript of the article published in final edited form as: Famoso, F., Wilson, J., Monforte, P., Brusca, S., & Lulla, V. (2017). Measurement and modeling of ground-level ozone concentration in Catania, Italy using biophysical remote sensing and GIS. International Journal of Applied Engineering Research, 12, 10551–10562.

were active from 1992-2009. The number was reduced to six in 2010-11 and to only three in 2014 (Lanzafame et al., 2014 and Famoso et al., 2015). This decline in monitoring sites reduces the potential to examine spatial and temporal variations of intra-urban air quality and localized exposures to sensitive populations.

Spatial variation in ground-level O_3 was evaluated in the current study using a network of thirty passive samplers deployed in a 6x5 500m grid pattern covering sections of Catania's urban core and periphery. Biophysical measures derived from satellite imagery and built environment characteristics from GIS sources were evaluated as correlates and used to develop a land use regression (LUR) model that explained 74% of the variation (adjusted R^2) in measured O_3 concentration across the study area.

BACKGROUND

Study area

Catania is the second largest city in Sicily, Italy with approximately 315,000 inhabitants in the city proper and of over 1 million in the metropolitan area. The city's population density is about 1,745 people/km^2 with the highest density occurring near the historic center (ISTAT population census 2011). Geographically, Catania is situated at the base of Mt. Etna on the Ionian Sea, a setting that creates marine breezes and ventilation regimes that contribute to air pollutant dispersion for most days of the year (Lanzafame et al., 2014; Famoso et al., 2015). This compensates partially for the negative effects of the intense private vehicular traffic and old vehicle fleet. About 65,000 vehicles per day travel in the center of the city, creating chaotic traffic conditions that are exacerbated by a dense road pattern. Public transportation systems do not serve all parts of the metropolitan area therefore transportation demand is satisfied primarily by private vehicles. The result is frequent traffic congestion, peaking during morning and evening commutes. While Catania's pollutions levels measured at the official monitoring do not usually exceed the limits set by European directive 2008/50 CE, deterioration of air quality during peak traffic is a constant problem in the city (Lanzafame et al., 2014; Lanzafame et al., 2015).

Previous research

Land use regression (LUR) models are commonly used to estimate spatial patterns of air pollutants based on measured values at sampling locations and a set of independent variables (Jerrett et al., 2005; Hoek et al., 2008; Adam-Poupart et al., 2014). Recent review articles reveal a range of methodological variations and predictor variables (Ryan and LeMasters, 2007; Hoek, 2008; Gulliver 2012; Gulia et al., 2015). Variables related to motor vehicle traffic are common because it is a principal source of pollution in urban areas, though fixed-point sources (e.g., factories, refineries and powerplants) may contribute significantly in some contexts. Transportation variables including road class, length and density, traffic volume, and vehicle counts are common. Other variables commonly used include population density, land use and land cover, physical geography (e.g., altitude, latitude/longitude, distance to major water bodies), and meteorological or climatic variables. However, variables and their specific definitions can vary across studies as a result of differences in data availability, study objectives, and unique local characteristics.

Direct measurement of air pollutants from satellites is an active area of research, but atmospheric optical properties and the spatial resolution of sensors designed specifically for air quality monitoring present challenges to spatially detailed intra-urban applications (Loughner et al., 2007; Martin, 2008; Knibbs et al., 2014; Brauer et al., 2015; Van Doneklaar et al., 2015). Despite the common use of land use and land cover data derived from remote sensing technology in air pollution LUR models (e.g., Novotny et al., 2011; Beelen et al., 2013), objective biophysical measurements from moderate and high-resolution satellites, such as land surface temperature (LST), albedo, and spectral indexes have not been widely investigated as predictor variables, though a few studies are present in the literature. For example, Thiering (2016) concluded that the normalized difference vegetation index (NDVI) (an indicator of photosynthetic biomass) measured within 0.5 and 1km buffers around subjects' residences was inversely associated with NO_2 and PM_{10} exposure. Mozumder et al. (2013) observed significant inverse relationships between air pollution index values when compared to near infrared reflectance and NDVI measured from satellite imagery. Dadvand et al. (2012) reported that NDVI had a significant inverse correlation with $PM_{2.5}$ levels when measured in 100, 200 and 250m buffers around study participants' home and work locations, but NDVI was not significantly associated with measured NO_x exposure.

Additional complexities in urban morphology that impact temperature and airflow including planimetric and 3D surface area of buildings, urban canyons, surface roughness, and predominant wind direction also affect pollutant concentration and dispersion (Oke, 1978; Souch and Grimmond, 2006; Krüger et al., 2011). For example, Su et al. (2008) reported that including building morphometric characteristics (height/width ratio of urban canyons) significantly improved LUR models, increasing the variance explained from 56% to 67% for NO_2, and from 72% to 85% for NO.

Another methodological issue associated with LUR models is defining the area of influence around sampling locations. A common approach is to use circular buffers at varying radii. For example, Madsen et al. (2007) used circular buffers ranging from 50 to 1000m to examine NO_x at 80 passive sampling locations in Oslo, Norway. Hoek et al. (2008) suggested that buffers should account for measured declines in the effects of traffic on air quality at distances ranging from 100m for major roads to 500m for highways. Li et al. (2015) reported that LUR models using semicircular buffers oriented towards the

predominate wind direction resulted in significantly higher R^2 values when compared to models based on circular buffers.

DATA AND METHODS

Passive samplers and O_3 measurement

For this experimental study, passive samplers were deployed at 30 sites for two, 2-week periods in December 2014 to estimate spatial variation in concentrations of ground-level O_3. The samplers measure pollutant concentrations without forced air intake and were deployed in containers that permit exposure to ambient air, but provide protection from environmental factors such as rain, excessive irradiation, and wind (Plaisance et al., 2004). The devices were located 2 to 3 m above the ground in sites free from obstacles. Samplers used in the current study were obtained from Passam Ag of Zurich, Switzerland who also conducted the laboratory analysis to determine O_3 concentrations. Technical aspects of the samplers are summarized in Table 1.

Table 1: Technical characteristics of passive O_3 samplers

Technical Characteristics	**Specifications**
Range [µg/m^3]	1- 200
Maximum exposure	10 days
Limit reliability [µg/m^3]	0.6
External influences	
Wind	< 10% up to 4-5 m/s
Temperature	No influence 5-40 °C
Humidity	No influence 20-80%
Uncertainty*	25% in 20-40 µg/m^3

* according GUM (ISO Guide to the expression of uncertainty in measurement)

The samplers contained polypropylene or fiberglass phials treated with compounds that react with O_3. Once the phial is opened a reaction between the compound and the air begins, creating a concentration differential between the interior and exterior. The physical principle is based on the passive diffusion of a gas toward an absorbent in accordance with Frick's law (1):

$$F = -D \frac{dC}{dL} \quad (1)$$

Where F is the molar flow rate, D is the diffusion coefficient, C is the concentration and L is the diffusion path [1]. The diffusion conditions are influenced by the length of the diffusion path, L [cm], and the transversal area, A [cm^2]. The mean concentration of the gas is given by the equation (2):

$$= \quad \frac{\cdot}{\cdot\cdot} \quad (2)$$

Where t [min] is the exposition time, Q [µg] is the total quantity of the absorbed gas by the phial (calculated with spectrophotometric analysis).

Passive samplers are recognized by European legislation as exploratory devices despite the fact they provide precise measures (Krupa et al., 2000). Recent experiments have demonstrated significant correlation between air pollutant concentrations measures with passive samplers and those collected from official continuous monitoring stations in Catania (Lanzafame et al., 2016). The advantages of using passive samplers include ease of use, the opportunity to conduct surveys over a wide area, small size compared to active samplers, no need of electrical supply, and relatively low costs. While passive samplers do not substitute the authorized pollutant monitoring systems, they do present an ideal solution to measure pollutant distributions in a specific geographical area (Pfeffer et al., 2010).

Remote sensing and GIS variables

Circular buffers at 50, 100, 150 and 200m radii were generated around GPS coordinates for each of the 30 sampling locations. Semicircular buffers were created at the same radii in 2D and 3D following the methods of Li et al. (2015) in which the orientation of the buffer is based on the predominant wind direction. Data on wind direction during the monitoring period were acquired from 31 weather stations distributed throughout the Catania metropolitan area. The average bearing was calculated across all weather stations for the monitoring period at 207.58 degrees. Semicircular 3D buffers oriented to this bearing were generated at height of 70m in order to encompass the tallest buildings in the study area (Figure 1).

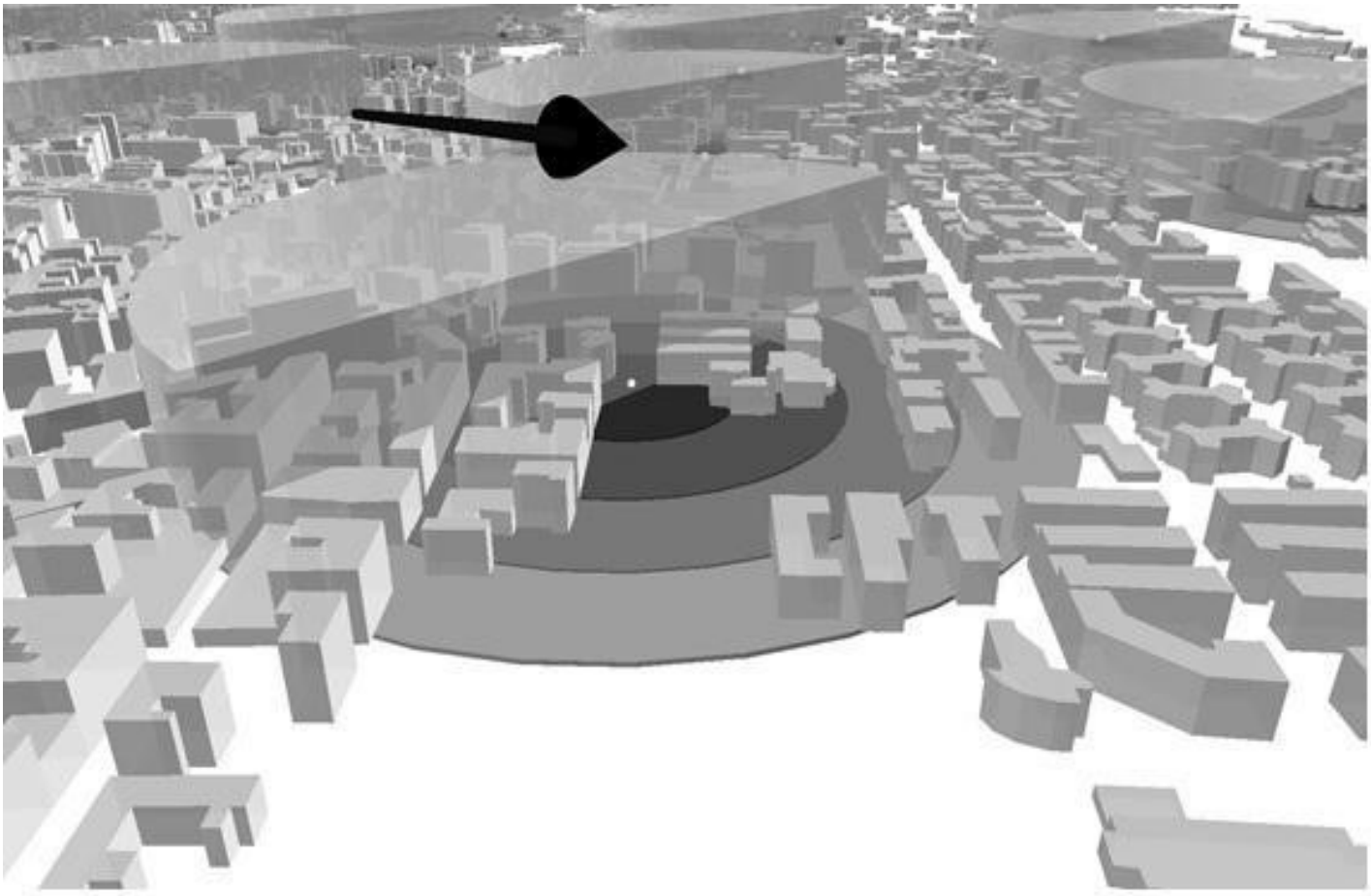

Figure 1: Example of 2d circular buffers (50, 100, 150 & 200m) and a 3D semicircular buffer (200m) based on predominate wind direction (black arrow) with 3D building model.

The US Geological Survey's EarthExplorer website (https://earthexplorer.usgs.gov/) was searched to identify could-free Landsat imagery of the study area acquired as close as possible in time to the air quality monitoring period. A cloud-free image captured by the Landsat 8 Operational Land Imager (OLI) and Thermal Infrared Sensor (TIRS) on 17 January 2015 (19 days after the monitoring period) was used to derive the remote sensing variables evaluated as potential predictors of ground-level O_3 (scene identifier: LC08_L1TP_188034_20150117_20170414_01_T1).

Satellite image data were retrieved in the Landsat 8 surface reflectance product format, which is preprocessed so that pixel values represent surface reflectance for the 30-meter reflective bands (1-7 & 9) and top of atmosphere brightness temperature for the thermal bands (10 & 11) (USGS, 2017). The thermal bands are resampled from 100 to 30m to match the spatial resolution of the multispectral bands. An operational advantage to using the surface reflectance product format is that calibration procedures to correct for atmospheric scattering and absorption have already been applied based on data obtained from the MODIS sensor (Vermote et al., 2016).

Several validated spectral indexes can be generated when retrieving Landsat 8 surface reflectance products. In the current study, an NDVI image was used to estimate spatial variation in vegetation density within the study area. Landsat 8 data cannot be used independently to derive precise measurements surface albedo because of the narrow field of view and the need to incorporate viewing geometries from different angles (Roy et al., 2014; Vermote et al., 2016). However, estimates of broadband albedo can be derived using methods developed by Liang (2000) for the Landsat 7 ETM+ sensor that were later adapted for the Landsat 8 OLI instrument (Makido et al., 2016; Naegeli et al., 2017). Band 10 data from the TIRS sensor was used estimate land surface temperature (LST) following the methods described by Estoque et al. (2017). Band 10 was selected because it records measurements in a lower atmospheric absorption region and is less affected by stray light artifacts compared to band 11 (Jiménez-Muñoz et al., 2014).

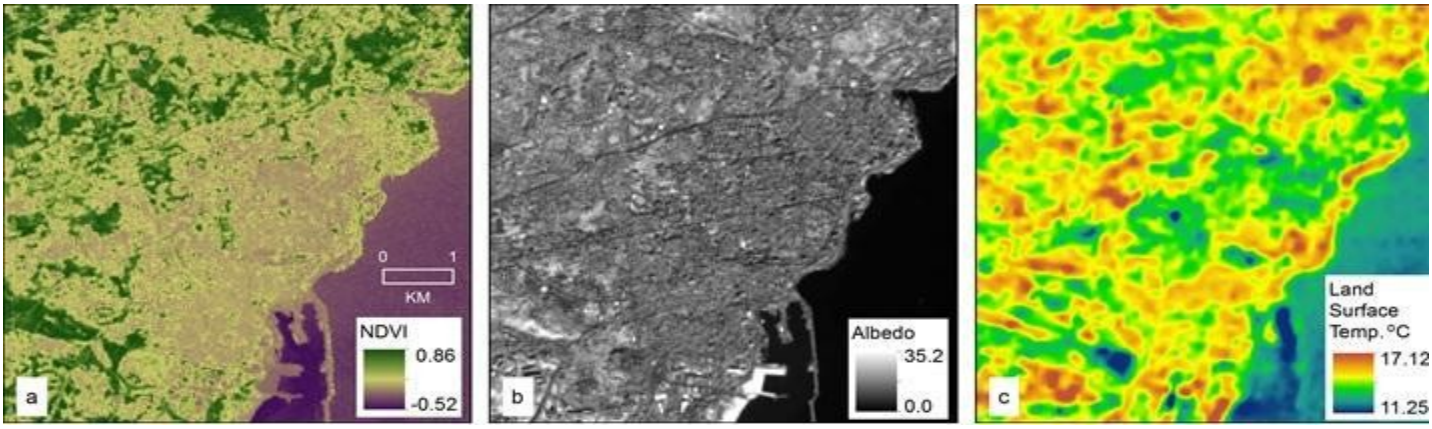

Figure 2: Biophysical remote sensing variables evaluated in LUR model. a) NDVI (normalized difference vegetation index), b) albedo, c) land surface temperature (LST).

GIS data from OpenStreetMap (OSM) were used to estimate road length in three classes (primary, secondary, and residential). From the same source (OSM) other variables were examined including counts of schools, garbage collection locations, rail stations, and bus stops in buffers surrounding monitoring locations. Building footprint data for the study area were acquired from Italy's National Geoportal (http://www.pcn.minambiente.it/). These data include a height attribute that was used in the current study to estimate 3D volume of buildings proximal to O_3 monitoring locations. Estimates of population density within each building were obtained from the Urbanism and Territorial Management Department of Catania.

Mean values of NDVI, albedo and LST were extracted within the circular and semicircular buffers around each monitoring location using zonal functions in a GIS. Similarly, GIS variables were summarized within the same buffers by count, total length, or area. Distance to the coast was defined as a continuous variable for each monitoring site.

Analysis methods

In total, 195 independent variables were generated when summarized in all buffer shapes and sizes. Similar to the methods applied by Briggs et al. (2000), Ross et. al (2007) and Meng et al. (2015), procedures in SPSS software were used to reduce the number of independent variables and find the best linear LUR model. First, a correlation matrix of the independent variables and the dependent variable was created. Variables with a correlation index < 0.20 were excluded. Preliminary collinearity tests were then applied to the remaining predictors by considering correlation indices > 0.50. The LUR model was developed using a stepwise approach. At each step, the independent variable not in the equation that had the smallest F statistic was entered. Variables already in the regression equation were removed if their F statistic became sufficiently large. As an entry F, "2" was used and as an as exit F "1" was used. The modelling process consisted of the following steps:

1. Exclude cases listwise. Only cases with valid values for all variables were included in the analyses.
2. Test for normality using ANOVA.
3. Test for collinearity between the independent variables. Eigenvalues of the scaled and uncentered cross-products matrix, condition indices, and variance-decomposition proportions were displayed along with variance inflation factors (VIF) and tolerances (T) for individual variables. T > 0.2 and VIF < 10 were used as thresholds.
4. Apply Durbin-Watson test to detect autocorrelation of model residuals.

The final model was selected by considering a combination of three parameters: $R^{adjusted}$, SE and the number of independent variables.

RESULTS

Measurements O_3 concentrations are shown in figure 3. The average was 26.55 $\mu g/m^3$ with a SD of 6.9 $\mu g/m^3$ (25.98%) demonstrating that the variation of was statistically significant. The overall pattern suggests higher concentrations in the peripheral areas of the city characterized by more open spaces and vegetation cover (see upper left inset), possibly due to increased solar insolation in these areas. None of the measured concentrations exceeded the official limit imposed by European Directive 2008/50/EC (Maximum daily 8-hour mean < 120 $\mu g/m^3$). Despite being below the official limits, some of the measured concentrations were relatively high for winter and were comparable to observations from other urban areas characterized by high air pollution, such as Delhi where winter values average around 40 $\mu g/m^3$ (Sharma et. al., 2016).

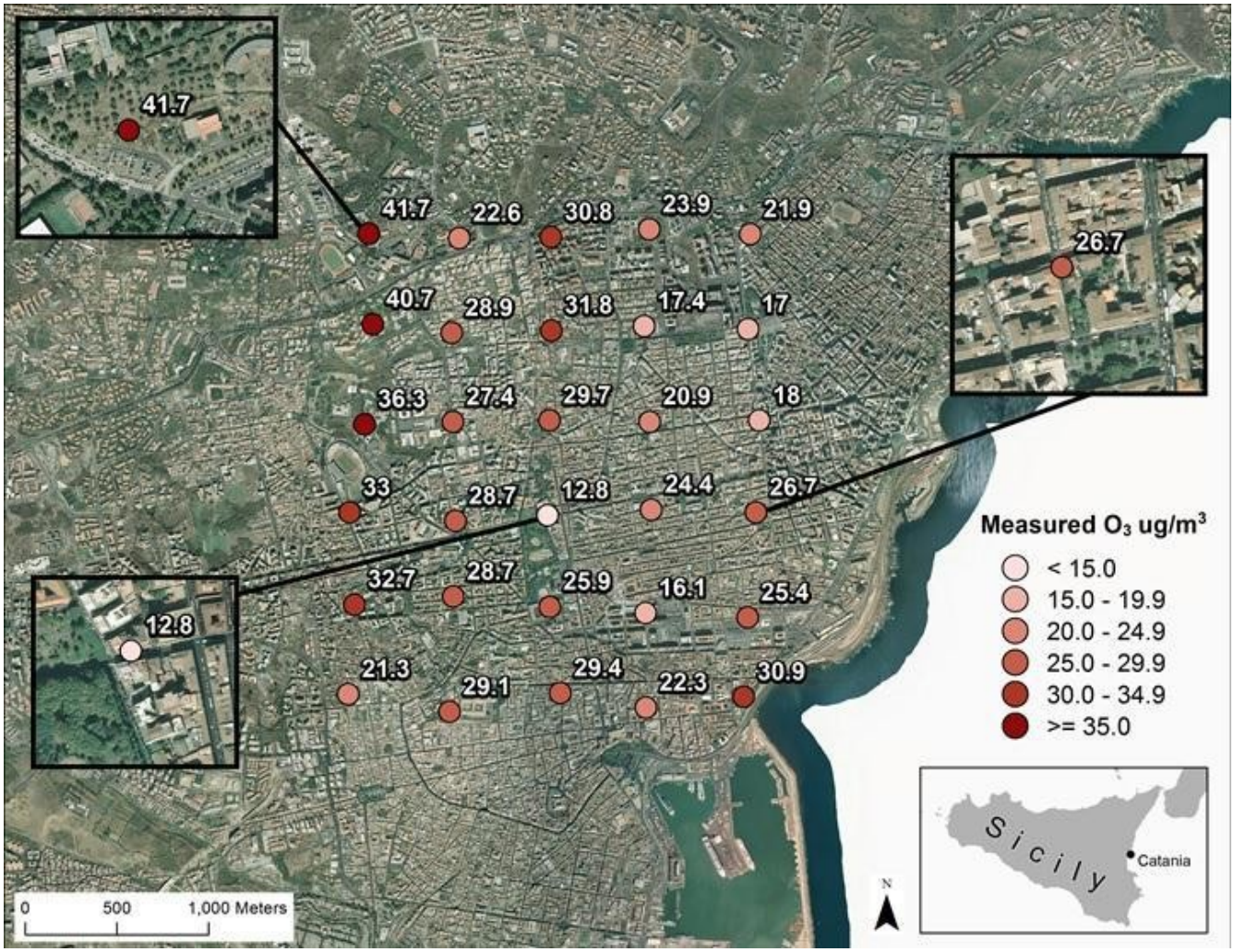

Figure 3: Passive sampling locations with measured O_3 concentrations ($\mu g/m^3$).

Table 2 lists the independent variables that had Pearson correlation coefficients > 0.50 with measured O_3 concentrations. All of the highly correlated variables, except for distance from the coast, were derived from remote sensing imagery. In particular, land surface temperature (LST) in almost all buffer variations was highly correlated with O_3 concentrations. This may be due to the causal links between temperature and ozone production. Albedo was also significantly correlated with O_3, possibly due to the relation between ultraviolet solar radiation and ozone formation. Several of the variables highly correlated with measured O_3 concentrations were derived within semicircular buffers rather than circular buffers, demonstrating the potential importance of considering predominant wind direction as suggested by Li et al. (2015).

Table 2: Independent variables with correlation coefficients > 0.50.

Ozone (O_3)	Pearson's *r*
LST_{200sc}	0.734
LST_{150sc}	0.706
ALB_{200c}	0.686
LST_{100sc}	0.651
ALB_{150c}	0.632
ALB_{100c}	0.630
ALB_{200sc}	0.627
LST_{200c}	0.614
LST_{150c}	0.604
LST_{100c}	0.564
LST_{50sc}	0.558
ALB_{150sc}	0.517
LST_{50c}	0.513
Coast	0.506

Based on the regression methods described previously, the best linear model was derived using four variables and one constant:

O_3 concentration = **-112.327** + **0.003** Coast + **0.021**$Rlength_{50c}$ – **0.001** $Buildings_{50c}$ + **9.473**LST_{200sc}

As shown by table 3, the dependent variables selected in the final LUR model did not exhibit significant collinearity. The correlation of them with Ozone is high in almost all cases, in particular the most correlated is LST_{sc200} with a positive correlation very close to 1 (0.734). The positive and high value demonstrates that the land surface temperature has a high impact in the formation of ozone.

The Euclidean distance of sampling locations to the coast was another important predictor. The positive value (0.506) may be a function of more congested traffic areas that are located further from the coast. Moreover, the microclimatic changes that occur between the more humid zones close to the coast and the drier zones far from the coast may be another explanation.

Given that ozone precursors are predominantly emitted during the combustion of fossil fuels, increased vehicular traffic is positively correlated with ozone. This is possibly reflected in the positive correlation (0.319) between total lengths of residential streets in 50m buffers around the sampling locations. Residential streets in the city are typically characterized by more congested traffic in urban canyons. The last predictor in the model is the total area of buildings (m^2) calculated in the buffer of 50 m. The negative Pearson coefficient observed may imply that ozone formation is more facilitated in higher insolation and less shadow effects of surrounding buildings.

Table 4 summarizes characteristics of the LUR model. All variables presented low variance inflation factors (VIFs) and tolerance statistics, which further demonstrate low collinearity among predictor variables. The standardized coefficients suggest the most important variable was LST_{200sc} with a β of 0.657, almost three times higher than the other variables. Overall, the model was able to explain almost 80% the variation in measured O_3 concentrations (R^2=0.775, adjusted R^2=0.739). The Durbin-Watson index of 2.188 indicated there is neither positive nor negative spatial autocorrelation between residuals and they follow a normal distribution (Figure 4).

Table 3: Pearson correlation coefficients between significant variables in the final LUR model.

Variables	Ozone (O_3)	Coast distance	Res length_c50	buildings_c50	LST_sc200
Ozone (O_3)	1	0.506	0.319	-0.272	0.734
Coast distance		1	0.178	-0.271	0.158
Res length_c50			1	0.245	0.141
buildings_c50				1	0.008
LST_sc200					1

Table 4: Summary of final land use model indices.

	Unstandardized Coefficients		Standardized Coefficients	Collinearity Statistics	
Model predictors	β	Std. Error	β	Tolerance	VIF
Intercept	-112.327	19.797			
Coast_Distance	0.003	0.001	0.290	0.847	1.180
Res length_c50	0.021	0.009	0.238	0.866	1.155
buildings_c50	-0.001	0.001	-0.257	0.837	1.194
LST_sc200	9.473	1.397	0.657	0.962	1.040
Model summary	R	R^2	Adjusted R^2	Std. Error of Estimate	Durbin-Watson
	0.88	0.775	0.739	3.531	2.188
Residuals statistics	Std. mean Error of predicted value	Mean Mahal. Distance	Mean Cook's Distance		
	1.389	0.044	3.867		

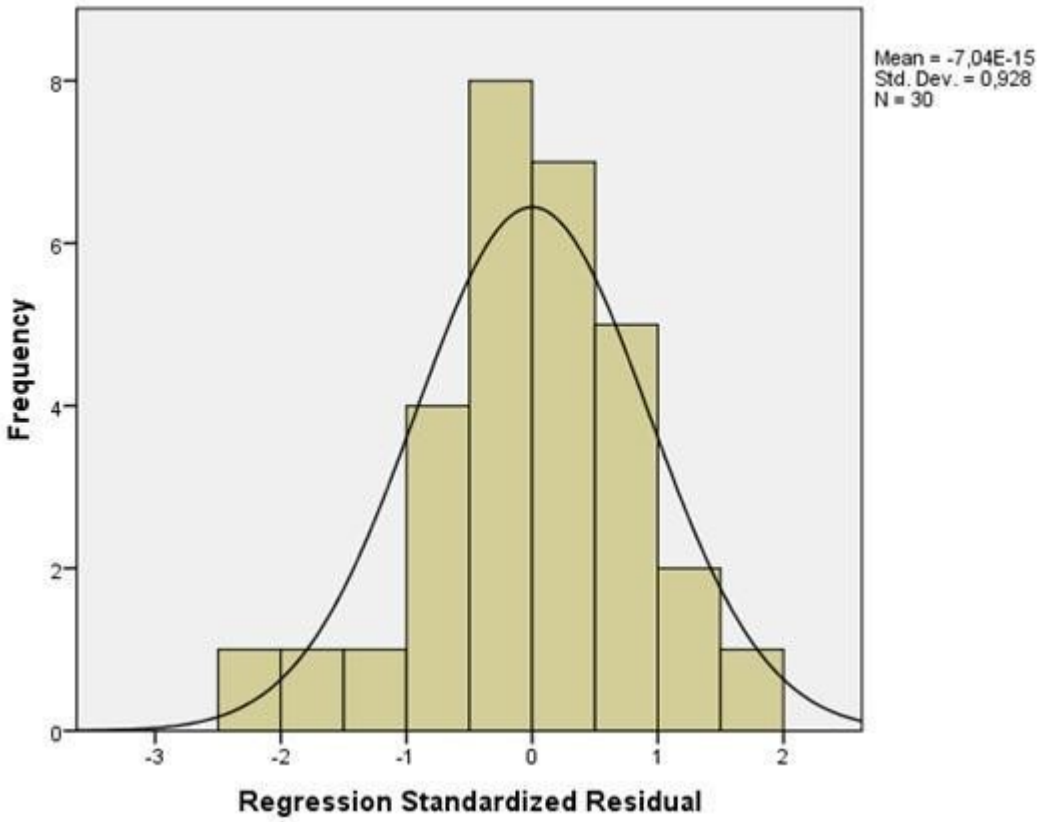

Figure 4: Frequency distribution of residuals.

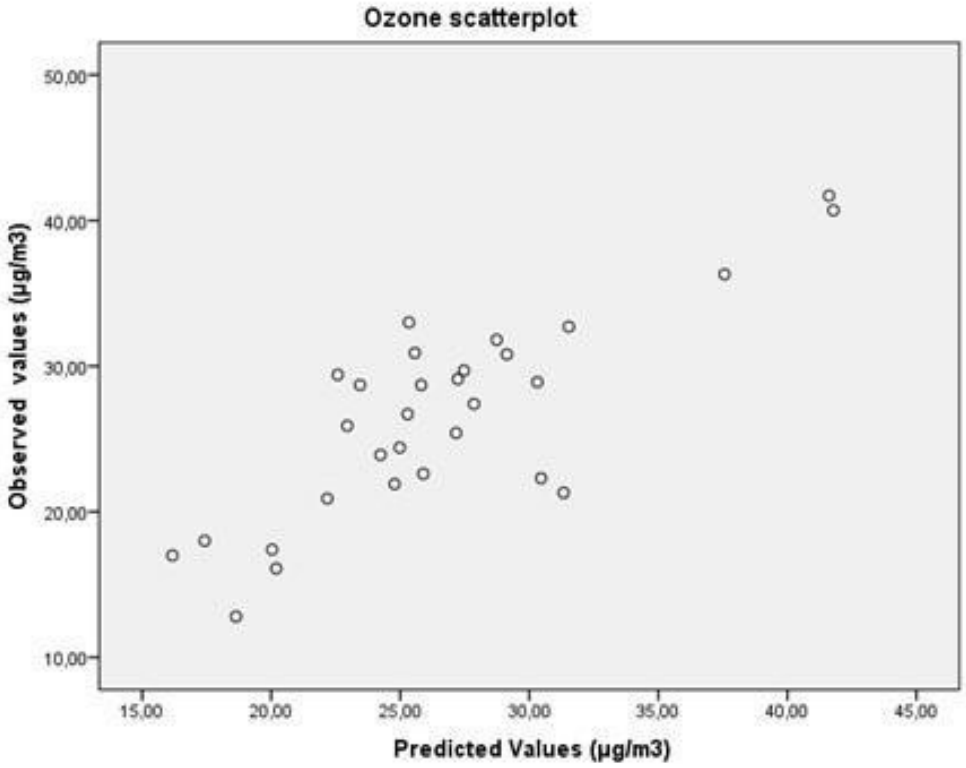

Figure 5: Observed vs. predicted ozone concentrations (ug/m^3).

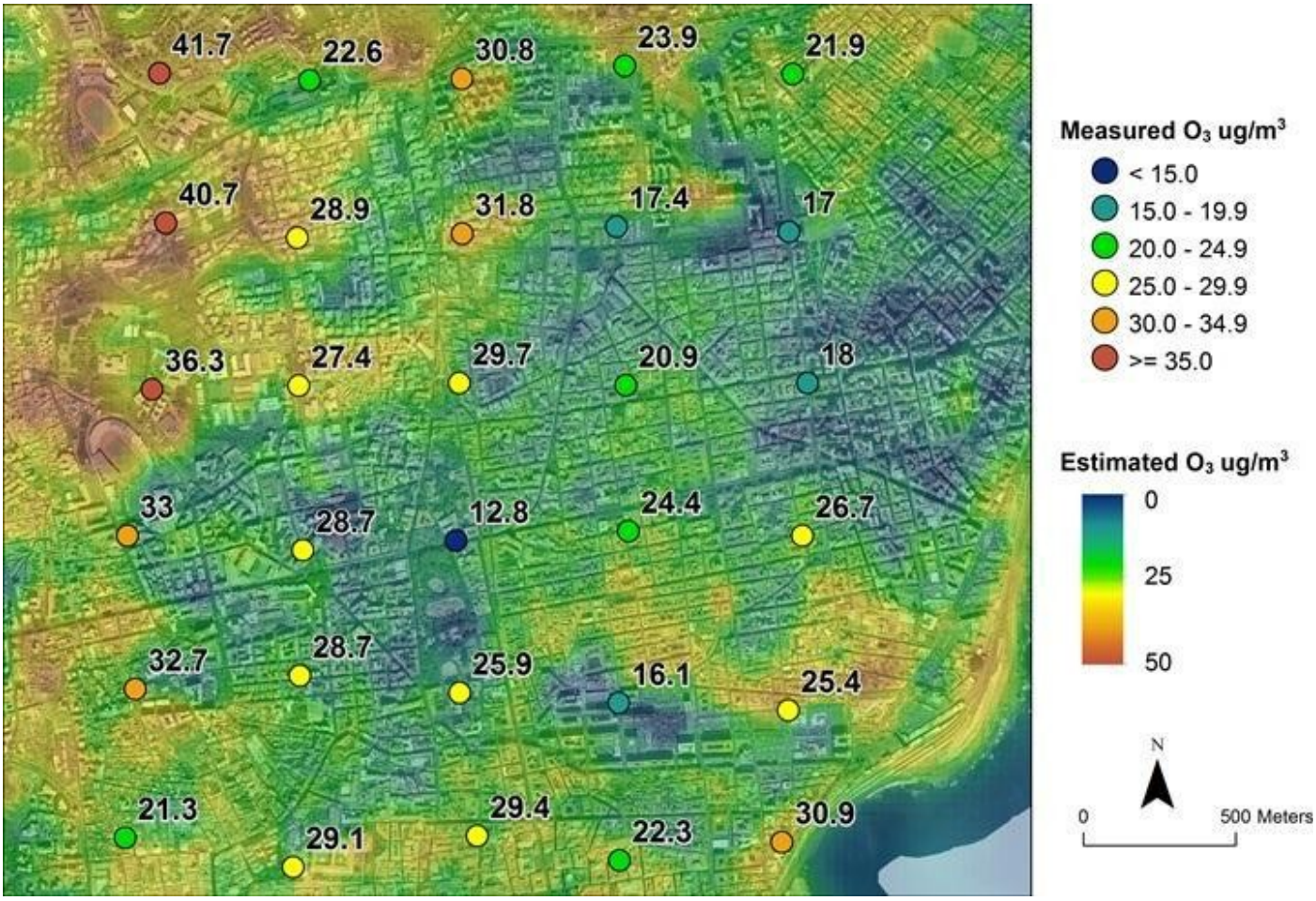

Figure 6: Passive sampling locations with measured O_3 and estimated O_3 from land use regression model.

CONCLUSIONS

The results of this study suggest that testing the utility of biophysical remote sensing measurements as correlates of urban air pollutants is a potentially important methodological research direction. Standardized products like the Landsat 8 surface reflectance imagery used in this study provide relevant data on biophysical parameters on a near global basis. The preprocessing also provides standardization that facilitates testing the transferability of models derived from these data to other spatial and temporal contexts. Importantly, image data to facilitate this research is freely accessible for most of the Earth's surface through sources such as the Landsat and other image archives.

Fewer studies have focused on measurement and modeling of intra-urban variations O_3 as compared to particulate matter (PM) and nitrous oxides (NO_x) (Malmqvist et al., 2014; Kerckhoffs et al., 2015).

The results of this exploratory study suggest several directions for future research on intra-urban variations in ground-level O_3. First, the monitoring results demonstrate that low-cost, passive samplers distributed in an objective grid pattern were able to detect significant spatial variation of O_3 concentrations in an urban environment. Second, results of the land use regression model indicated that objective measurements of biophysical variables from satellite imagery contribute significantly to explaining spatial variations in intra-urban O_3 concentrations. Additionally, independent variables summarized within semicircular buffers oriented to the prevailing wind direction tended to be more highly correlated with O_3 concentrations as compared to the measures summarized within circular buffers. This is consistent with the findings reported Li et al. (2015).

Limitations of this exploratory study included the short sampling period, the relatively small number of sampling locations, and lack of validation monitoring sites. However, the initial results suggest further examination of biophysical remote sensing variables as inputs to LUR models examining intra-urban patterns of ground-level O_3 and potentially other pollutants are worthy of further investigation. Longer term sampling (i.e., repeated measures over the course of a year) integrating temporally coincident remote sensing data could strengthen the case for the results reported in the current study. The extendibility of these results also needs to tested in other locations and over time.

REFERENCES

[1] Adam-Poupart, A., Brand, A., Fournier, M., Jerrett, M., & Smargiassi, A. (2014). Spatiotemporal modeling of ozone levels in Quebec (Canada): a comparison of kriging, land-use regression (LUR), and combined Bayesian maximum entropy-LUR approaches. *Environmental Health Perspectives* (Online), 122(9), 970.

[2] Al-Hegelan, M., Tighe, R. M., Castillo, C., & Hollingsworth, J. W. (2011). Ambient ozone and pulmonary innate immunity. *Immunologic Research*, 49(1-3), 173-191.

[3] Beelen, R., Hoek, G., Vienneau, D., Eeftens, M., Dimakopoulou, K., Pedeli, X., Tsai, M.Y., Künzli, N., Schikowski, T., Marcon, A. and Eriksen, K.T. (2013). Development of NO 2 and NO x land use regression models for estimating air pollution exposure in 36 study areas in Europe–the ESCAPE project. *Atmospheric Environment*, 72, 10-23.

[4] Brauer, M., Freedman, G., Frostad, J., Van Donkelaar, A., Martin, R. V., Dentener, F., ... & Balakrishnan, K. (2015). Ambient air pollution exposure estimation for the global burden of disease 2013. *Environmental Science & Technology*, *50*(1), 79-88.

[5] Briggs, D. J., De Hoogh, C., Gulliver, J., Wills, J., Elliott, P., Kingham, S., Smallbone, K. (2000). A regression-based method for mapping traffic-related air pollution: application and testing in four contrasting urban environments. *Science of the Total Environment*, 253, 151-167.

[6] Calfapietra, C., Morani A, Sgrigna G., John S., Muzzini V., Pallozzi E., Guidolotti G., Nowak D., Fares S. (2016). Removal of ozone by urban and peri-urban forests: evidence from laboratory, field, and modeling approaches. *Journal of Environmental Quality*, 45 (1), 224-233.

[7] D'Amato, G., Cecchi, L., D'amato, M., & Liccardi, G. (2010). Urban air pollution and climate change as environmental risk factors of respiratory allergy: an update. Journal of Investigational Allergology and Clinical Immunology, 20(2), 95-102.

[8] Dadvand, P., de Nazelle, A., Triguero-Mas, M., Schembari, A., Cirach, M., Amoly, E., Figueras, F., Basagaña, X., Ostro, B. and Nieuwenhuijsen, M. (2012). Surrounding greenness and exposure to air pollution during pregnancy: an analysis of personal monitoring data. *Environmental Health Perspectives*, 120(9), 1286.

[9] Estoque, R. C., Murayama, Y., & Myint, S. W. (2017). Effects of landscape composition and pattern on land surface temperature: An urban heat island study in the megacities of Southeast Asia. *Science of the Total Environment*, *577*, 349-359.

[10] Famoso, F., Lanzafame, R., Monforte, P., Oliveri, C., & Scandura, P. F. (2015). Air quality data for Catania: Analysis and investigation case study 2012-2013. *Energy Procedia*, *81*, 644-654.

[11] Gulia, S., Shiva Nagendra, S. M., Khare, M., & Khanna, I. (2015). Urban air quality management-A review. *Atmospheric Pollution Research*, 6(2), 286–304.

[12] Hoek, G., Beelen, R., De Hoogh, K., Vienneau, D., Gulliver, J., Fischer, P., & Briggs, D. (2008). A review of land-use regression models to assess spatial variation of outdoor air pollution. *Atmospheric Environment*, 42(33), 7561-7578.

[13] Jerrett, M., Buzzelli, M., Burnett, R.T., & DeLuca, P.F. (2005). Particulate air pollution, social confounders, and mortality in small areas of an industrial city. *Social Science & Medicine*, *60*(12), 2845-2863.

[14] Jerrett, M., Brook, R., White, L.F., Burnett, R T., Yu, J., Su, J., Seto, E., Marshall, J., Palmer, J.R., Rosenberg, L., & Coogan, P.F. (2017). Ambient ozone and incident diabetes: A prospective analysis in a large cohort of African American women. *Environment International*, 102, 42–47.

[15] Jiménez-Muñoz, J. C., Sobrino, J. A., Skokoviٕ, D., Mattar, C., & Cristóbal, J. (2014). Land surface temperature retrieval methods from Landsat-8 thermal infrared sensor data. *Geoscience and Remote Sensing Letters, IEEE*, 11(10), 1840–1843

[16] Kerckhoffs, J., Wang, M., Meliefste, K., Malmqvist, E., Fischer, P., Janssen, N.A., Beelen, R. and Hoek, G. (2015). A national fine spatial scale land-use regression model for ozone. *Environmental Research*, *140*, 440-448.

[17] Knibbs, L. D., Hewson, M. G., Bechle, M. J., Marshall, J. D., & Barnett, A. G. (2014). A national satellite-based land-use regression model for air pollution exposure assessment in Australia. *Environmental research*, *135*, 204-211.

[18] Krüger, E. L., Minella, F. O., & Rasia, F. (2011). Impact of urban geometry on outdoor thermal comfort and air quality from field measurements in Curitiba, Brazil. *Building and Environment*, 46(3), 621–634.

[19] Krupa, S. V., Legge, A. H. (2000). Passive sampling of ambient, gaseous air pollutants: an assessment from an ecological perspective. Environmental Pollution, 107, 31-45.

[20] Lanzafame, R., Scandura, P. F., Famoso, F., Monforte, P., & Oliveri, C. (2014). Air Quality Data for Catania:

Analysis and Investigation Case Study 2010–2011. Energy Procedia, 45, 681-690.

[21] Lanzafame, R., Monforte, P., Patanè, G., & Strano, S. (2015). Trend analysis of Air Quality Index in Catania from 2010 to 2014. Energy Procedia, 82, 708-715.

[22] Lanzafame, R., Monforte, P., & Scandura, P. F. (2016). Comparative analyses of urban air quality monitoring systems: passive sampling and continuous monitoring stations. Energy Procedia, 101(2), 321–328.

[23] Li, X., Liu, W., Chen, Z., Zeng, G., Hu, C., León, T., Liang, J., Huang, G., Gao, Z., Li, Z. and Yan, W. (2015). The application of semicircular-buffer-based land use regression models incorporating wind direction in predicting quarterly NO2 and PM10 concentrations. *Atmospheric Environment*, 103, 18–24.

[24] Liang, S. (2000). Narrowband to broadband conversions of land surface albedo I: Algorithms. *Remote Sensing of Environment*, 76(2), 213-238.

[25] Loughner, C. P., Lary, D. J., Sparling, L. C., Cohen, R. C., DeCola, P., & Stockwell, W. R. (2007). A method to determine the spatial resolution required to observe air quality from space. *IEEE Transactions on Geoscience and Remote Sensing*, 45(5), 1308-1314.

[26] Madsen, C., Carlsen, K.C.L., Hoek, G., Oftedal, B., Nafstad, P., Meliefste, K., Jacobsen, R., Nystad, W., Carlsen, K.H. and Brunekreef, B. (2007). Modeling the intra-urban variability of outdoor traffic pollution in Oslo, Norway—A GA 2 LEN project. *Atmospheric Environment*, 41(35), 7500-7511.

[27] Malmqvist, E., Olsson, D., Hagenbjörk-Gustafsson, A., Forsberg, B., Mattisson, K., Stroh, E., Strömgren, M., Swietlicki, E., Rylander, L., Hoek, G. and Tinnerberg, H. (2014). Assessing ozone exposure for epidemiological studies in Malmö and Umeå, Sweden. *Atmospheric Environment*, *94*, 241-248.

[28] Martin, R. V. (2008). Satellite remote sensing of surface air quality. *Atmospheric Environment*, 42(34), 7823-7843.

[29] Makido, Y., Shandas, V., Ferwati, S., & Sailor, D. (2016). Daytime variation of urban heat islands: the case study of Doha, Qatar. *Climate*, 4(2), 32.

[30] Meng, X., Chen, L., Cai, J., Zou, B., Wu, CF., Fu, Q., Zhang, Y., Liu, Y., Kan, H. (2015). A land use regression model for estimating the NO2 concentration in shanghai, China. Environmental Research, 137, 308-315.

[31] Monn, C. (2001). Exposure assessment of air pollutants: a review on spatial heterogeneity and indoor/outdoor/personal exposure to suspended particulate matter, nitrogen dioxide and ozone. *Atmospheric Environment*, *35*(1), 1-32.

[32] Mozumder, C., Reddy, K. V., & Pratap, D. (2013). Air pollution modeling from remotely sensed data using regression techniques. *Journal of the Indian Society of Remote Sensing*, 41(2), 269-277.

[33] Naegeli, K., Damm, A., Huss, M., Wulf, H., Schaepman, M., & Hoelzle, M. (2017). Cross-comparison of albedo products for glacier surfaces derived from airborne and satellite (Sentinel-2 and Landsat 8) optical data. *Remote Sensing*, 9(2), 110.

[34] Novotny, E. V., Bechle, M. J., Millet, D. B., & Marshall, J. D. (2011). National satellite-based land-use regression: NO_2 in the United States. *Environmental Science & Technology*, 45(10), 4407-4414.

[35] Oke, T. R. (1978). *Boundary Layer Climates*, 372 pp. Methuen, New York.

[36] Plaisance, H., Piechocki-Minguy, A., Garcia-Fouque, S., & Galloo, J. C. (2004). Influence of meteorological factors on the NO 2 measurements by passive diffusion tube. *Atmospheric Environment*, 38(4), 573-580.

[37] Pfeffer, U., Zang, T., Rumpf, E. M., & Zang, S. (2010). Calibration of diffusive samplers for nitrogen dioxide using the reference method–Evaluation of measurement uncertainty. *Gefahrstoffe, Reinhaltung der Luft*, 11(12), pp.500-506.

[38] Ross, Z., Jerret, M., Ito, K., Tempalski, B., Thurston, G.D. (2007). A land use regression for predicting fine particulate matter concentrations in the New York City region. *Atmospheric Environment*, 41, 2255-2269.

[39] Ryan, P. H., & LeMasters, G. K. (2007). A review of land-use regression models for characterizing intraurban air pollution exposure. *Inhalation Toxicology*, 19(sup1), 127-133.

[40] Roy, D.P., Wulder, M.A., Loveland, T.R., Woodcock, C.E., Allen, R.G., Anderson, M.C., Helder, D., Irons, J.R., Johnson, D.M., Kennedy, R. and Scambos, T.A. (2014). Landsat-8: Science and product vision for terrestrial global change research. *Remote Sensing of Environment*, 145, 154-172.

[41] Sharma, S., Sharma, P., Khare, N., Kwatra, S. (2016). Statistical behavior of ozone in urban environment. *Sustainable Environment Research,* 26(3), 142-148.

[42] Souch, C., & Grimmond, S. (2006). Applied climatology: urban climate. *Progress in Physical Geography*, 30(2), 270-279.

[43] Su, J. G., Brauer, M., & Buzzelli, M. (2008). Estimating urban morphometry at the neighborhood scale for improvement in modeling long-term average air

pollution concentrations. *Atmospheric Environment*, 42(34), 7884-7893.

[44] Thiering, E., Markevych, I., Brüske, I., Fuertes, E., Kratzsch, J., Sugiri, D., Hoffmann, B., von Berg, A., Bauer, C.P., Koletzko, S. and Berdel, D. (2016). Associations of residential long-term air pollution exposures and satellite-derived greenness with insulin resistance in German adolescents. *Environmental Health Perspectives*, 124(8), 1291.

[45] USGS (United States Geological Survey) (2017). Product Guide: Landsat 8 Surface Reflectance Code (LASRC) Product, (Version 3.8). 38 pp. https://landsat.usgs.gov/sites/default/files/documents/lasrc_product_guide.pdf

[46] Van Donkelaar, A., Martin, R. V., Brauer, M., & Boys, B. L. (2015). Use of satellite observations for long-term exposure assessment of global concentrations of fine particulate matter. *Environmental Health Perspectives*, 123(2), 135.

[47] Vermote, E., Justice, C., Claverie, M., & Franch, B. (2016). Preliminary analysis of the performance of the Landsat 8/OLI land surface reflectance product. *Remote Sensing of Environment*, 185, 46-56.